

Review

Overview on Photoreforming of Biomass Aqueous Solutions to Generate H₂ in the Presence of g-C₃N₄-Based Materials

E. I. García-López ^{1,*}, L. Palmisano ²  and G. Marci ² 

¹ Department of Biological, Chemical and Pharmaceutical Sciences and Technologies (STEBICEF), University of Palermo, Viale delle Scienze, 90128 Palermo, Italy

² “Schiavello-Grillone” Photocatalysis Group, Department of Engineering, University of Palermo, Viale delle Scienze, 90128 Palermo, Italy

* Correspondence: elisaisabel.garcialopez@unipa.it

Abstract: Photoreforming (PR) of biomass can be considered a viable technology under mild experimental conditions to produce hydrogen with a high reaction rate using compounds from renewable resources and waste materials. The application of biomass PR gives rise to both hydrogen generation and biomass waste valorization. The process could be scaled up to obtain hydrogen under natural sunlight irradiation, and research on polymeric carbon nitride (g-C₃N₄)-based photocatalysts has been widely carried out in recent years. The non-metallic-based carbon nitride materials are economical and (photo)stable polymer semiconductors, and their physicochemical surface and electronic properties are optimal for obtaining H₂, which can be considered a gas that does not cause major environmental problems. Some hindrances related to their structure, such as the low absorption of visible light and the relatively high recombination rate of electron-hole pairs, restrict the performance; therefore, it is necessary to improve their activity and the yield of the reaction by modifying them in various ways. Various types of solutions have been proposed in this regard, such as, for example, their coupling with other semiconductors to form composite materials. The current mini-review aims to overview the PR field, reporting some of the most interesting papers devoted to understanding the role of g-C₃N₄ in biomass PR. Information on many physico-chemical aspects related to the performance of the process and possible ways to obtain better results than those present up to now in the literature will be reported.

Keywords: polymeric carbon nitride; C₃N₄; H₂; hydrogen production; photoreforming; biomass; photocatalysis



Citation: García-López, E.I.; Palmisano, L.; Marci, G. Overview on Photoreforming of Biomass Aqueous Solutions to Generate H₂ in the Presence of g-C₃N₄-Based Materials. *ChemEngineering* **2023**, *7*, 11. <https://doi.org/10.3390/chemengineering7010011>

Academic Editor: Dmitry Yu. Murzin

Received: 3 January 2023

Revised: 31 January 2023

Accepted: 1 February 2023

Published: 3 February 2023



Copyright: © 2023 by the authors. Licensee MDPI, Basel, Switzerland. This article is an open access article distributed under the terms and conditions of the Creative Commons Attribution (CC BY) license (<https://creativecommons.org/licenses/by/4.0/>).

1. Introduction

The significant rise of the Earth’s inhabitants and industrial progress has led to increasingly greater use of fossil fuels, with consequent depletion of energy resources and built up of environmental pollution.

Hydrogen is a fuel with a high calorific value (142 MJ·kg^{−1}) which is storable (although some precautions are necessary), clean and ecological, and its combustion leads to the formation of water without coproduction of other gases such as CO₂ or particulate matter [1]. It is predicted to be one of the most important energy carriers of the future and has been produced worldwide in recent years, mainly from steam reforming of natural gas, coal, or crude oil, and only a very small proportion has derived from biofuel reforming and electrolysis [2]. Thermal catalytic reforming of fossil fuels, mainly hydrocarbons, represents the most important source of hydrogen (about 95%), while the alternative use of biomass can be conceived as a second-generation technology. However, a large amount of heat required for the thermal catalytic reforming processes of aqueous solutions of organic compounds is a major obstacle to environmental sustainability; therefore, the development of technologies capable of exploiting solar energy and renewable raw materials to obtain green hydrogen from renewable resources such as water and biomass are welcome [3].

Heterogeneous photocatalysis can play an essential role in the progress of sustainable energy, and it is considered one of the best strategies for transforming solar energy into chemical energy. It is a green and low-cost technology that has demonstrated its potential use for environmental remediation, even if no large-scale applications have been realized and only niche applications can be hypothesized [4]. Since 1972, when Fujishima and Honda reported the possibility of obtaining “green” H_2 by the water-splitting process using a TiO_2 electrode under simulated solar irradiation [5], interest in this technology has increased tremendously. Green hydrogen can be obtained not only by photocatalytic water splitting but also by the photoreforming (PR) of an organic or inorganic substrate.

The photocatalytic reactions are started by the excitation of a semiconductor, which, when exposed to light having an energy equal to or greater than its band gap, causes the promotion of electrons (e^-) from the valence band (VB) to the conduction band (CB). The electron-hole pairs formed can recombine, release energy, or migrate and be trapped by active sites present on the semiconductor surface or by adsorbed species that are reduced or oxidized.

Figure 1 reports three important heterogeneous photocatalytic processes. Their application to water and air remediation has been largely studied [4]. The figure shows the classical application of the photocatalytic technology where the photoproduced electron-hole pairs must give rise to oxidation and a reduction reaction, respectively. The positive holes can react with donor species, often water molecules, which form very oxidant hydroxyl radicals ($\cdot OH$), and contemporaneous electrons can react with adsorbed molecules, usually O_2 , because the organic photo-oxidation processes are generally carried out in the air. Consequently, O_2 present in the air can react with electron-producing $\cdot O_2^-$ which in turn reacts with water-affording hydroxyl and hydroperoxide ($\cdot OOH$) radicals. The oxidant species formed unselectively react, giving rise to intermediates and, ultimately, the final products, which are mainly CO_2 and H_2O when the organic molecules in the suspension of the semiconductor only contain C and H. Notably, sulfates or nitrates can be formed from the mineralization of the organic substrate. Under anaerobic conditions, the splitting of water can produce H_2 and O_2 in a process called water photosplitting. This occurs when the energy of the electrons is sufficient to reduce protons to H_2 , i.e., when $E_{CB} < E_{(H_2/H^+)}$, and holes can oxidize water to O_2 , i.e., when $E_{VB} > E_{(O_2/H_2O)}$. Instead of H_2O , an organic molecule can act as a hole trap, and, therefore, the photogenerated holes, which act directly or indirectly through the production of hydroxide radicals, can lead to the production of a partially oxidized derivative of the organic molecule or to its complete decomposition to CO_2 and H_2O . This process, which uses organic molecules as traps for holes, is called photoreforming (PR). In this case, the organic species can be a biomass derivative, which is represented in Figure 1 simply as an organic molecule. Figure 1 also shows merely the photocatalytic oxidation of an organic molecule in the presence of oxygen, and this type of reaction has been studied extensively with the aim of breaking down polluting organic molecules. In the last case, the difference with respect to the photoreforming process is that in the organic photo-oxidation process, the molecular oxygen acts as an electron trap instead of water or protons (as shown in Figure 1), and, consequently, H_2 is not formed.

Indeed, the reduction of water or H^+ takes place only under anaerobic conditions and always gives rise to the formation of H_2 , as shown in Figure 1. Many articles claim to perform “water splitting” despite the fact that an organic species has been used as a hole scavenger; however, when O_2 (from water oxidation) is not obtained, it is more correct to refer to these reactions as PR instead of water splitting, as often reported in the literature [7]. Despite its attractiveness, water photo-splitting is a more difficult reaction than PR, both thermodynamically and kinetically. The H_2 formation rate is much higher in the PR process than in the photo-splitting one because the oxidation reaction of the organic species with photogenerated holes is irreversible. Conversely, H_2 and O_2 from water splitting can easily reform H_2O , decreasing the efficiency of converting light to hydrogen. The suppression of electron-hole recombination is also more difficult during the photo-splittingsplitting of water.

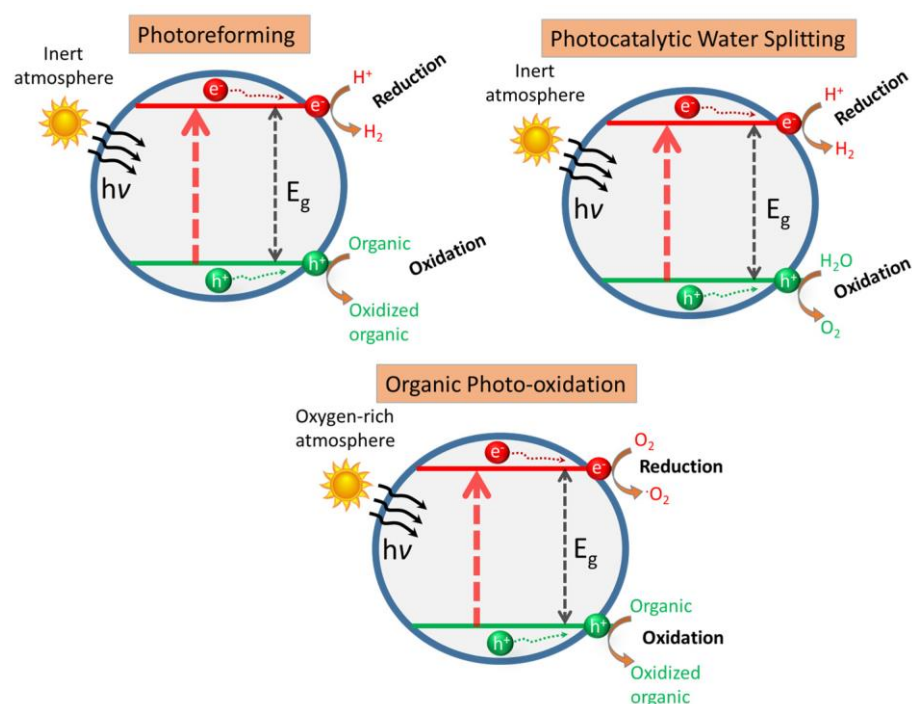
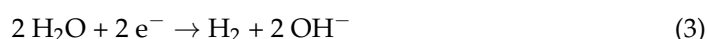


Figure 1. Reaction pathways of water photo-splitting and photoreforming under anaerobic conditions along with the oxidation of an organic molecule in the presence of oxygen. Reprinted with permission from Ref. [6].

The overall photocatalytic process to form H_2 can be considered for both water splitting and biomass PR. The splitting of water involves the concurrent **Oxygen Evolution Reaction (OER)** shown in Equation (1) and the **H_2 Evolution Reaction (HER)**, as reported in Equations (2) and (3):



or



with an overall process represented by Equation (4):

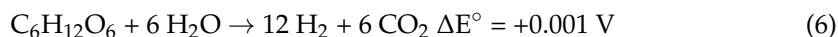
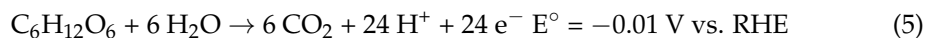


The highly reducing electrons can give rise to the hydrogen evolution reaction in Equations (2) and/or (3). As mentioned before, H_2 generation from water splitting possesses a large thermodynamic barrier due to the difficult oxygen evolution reaction (Equation (1)) with $E^\circ = +1.23 V$ vs. Normal Hydrogen Electrode (NHE) at $pH = 0$.

The PR process is considered non-selective and involves the splitting of water to generate H_2 through a reduction reaction and the simultaneous partial oxidation of an organic molecule to other species with higher added value or its mineralization to CO_2 and H_2O , all in one process. In PR, which must take place under anaerobic conditions, the electrons in the photocatalyst migrate to the (CB) and reduce the protons of H_2O to H_2 . The photogenerated holes in the (VB) of the photocatalyst (see Figure 1), on the other hand, oxidize the organic substrate.

The oxidizing species are the holes (h^+) in the VB, which can also form radical oxidizing species (reactive oxygen species, ROS), which in turn attack the biomass by oxidizing it as in the reaction shown in (Equation (5)) for glucose, where the latter molecule can obviously be considered only a model molecule representative of biomass. The overall PR process (Equation (6)) is, however, nearly energetically neutral ($\Delta E^\circ = +0.001 V$), which means

that energy is only needed to overcome the activation barriers. Thus, low-energy photons present in visible light that are very abundant in the solar spectrum can be used for biomass PR.

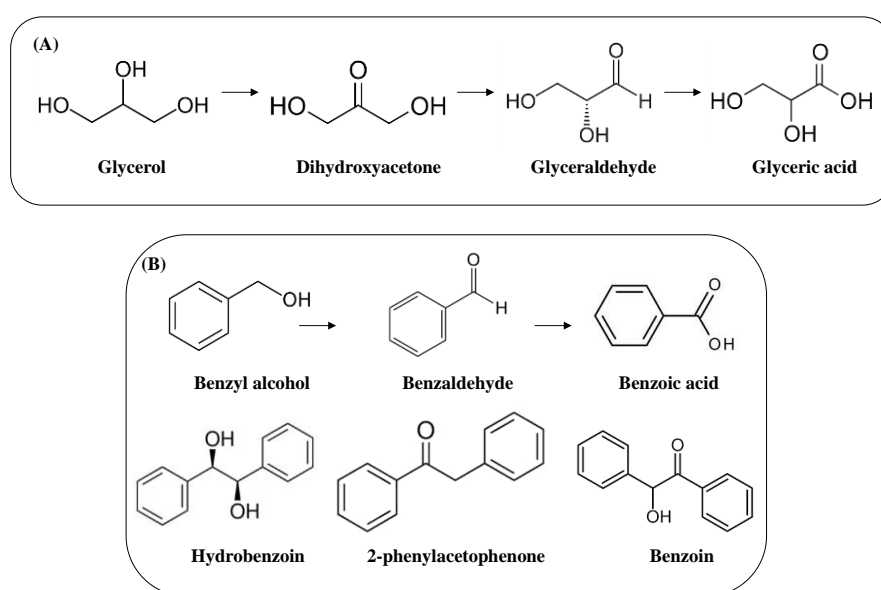


The effect of sacrificial reagents used as hole scavengers to boost hydrogen production was first reported in the 1980s by Kawai and Sakata [8]. Organic or inorganic species, including biomass compounds, may be used for the production of H_2 . Photoreforming has not received as much attention as water photo-splitting despite its interest and the high efficiencies reported. It is worth noting that its selectivity exceeds that of thermocatalytic processes due to the milder (environmental) conditions under which it proceeds, with comparable activity.

The idea is to obtain the desired products, possibly by increasing the selectivity toward the most interesting chemical, preventing the obtaining of dangerous or worthless compounds such as CO_2 . A mixture of various organic compounds is, therefore, undesirable. Toe et al. attribute the poor selectivity during PR to (i) unwanted adsorption/desorption of reacting species on the photocatalyst surface; (ii) uncontrolled formation of radical species (e.g., OH radicals) with a strong oxidant power; and (iii) saturation of the surface with products that gives rise to over-oxidation [9].

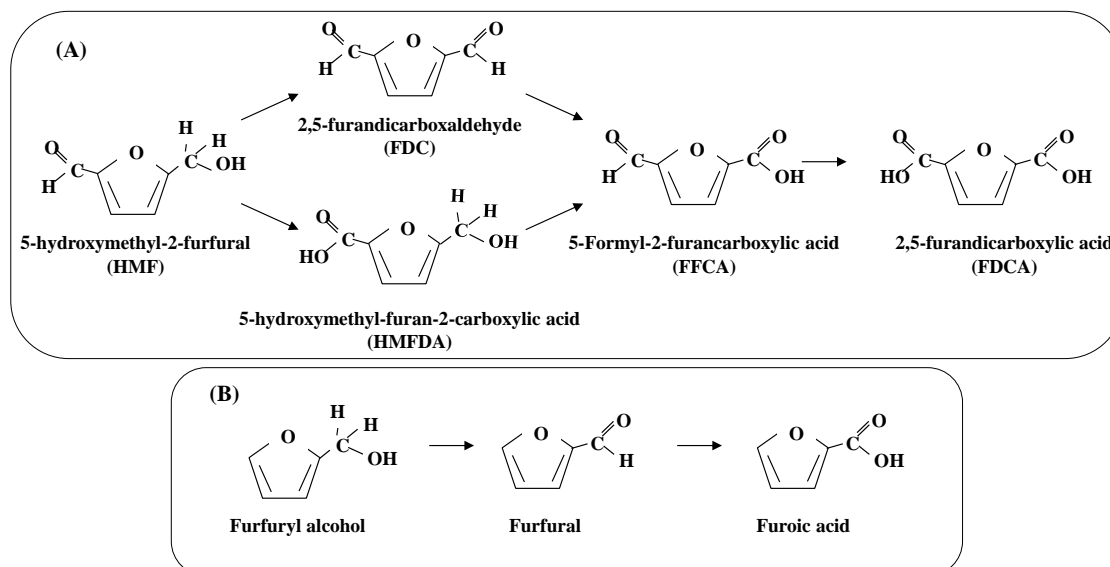
2. Organic Molecules as Hole Scavengers in Photoreforming: From Model Molecules to Biomass

Research on how to enhance selectivity toward photocatalytic organic transformation has long been studied, but mainly under aerobic conditions, where O_2 traps the electron from the conduction band. One of the most used organic substrates used for selective PR is methanol [10], whose partial oxidation gives rise to formaldehyde, formic acid, methyl formate, or ethylene glycol. Ethanol is also often used as a hole scavenger [11], forming mainly acetaldehyde, acetic acid, 1,1-diethoxyethane, and 2,3-butanediol. As shown in Scheme 1, when glycerol acts as a hole scavenger [12], dihydroxyacetone (DHA), glyceraldehyde, and glyceric acid are formed, while among the aromatics, benzyl alcohol gives rise to benzaldehyde, benzoic acid, hydrobenzoin, 2-phenylacetophenone, and benzoin.



Scheme 1. Partial oxidation products obtained from glycerol (A) and benzyl alcohol (B) as hole scavengers in the photoreforming reaction.

In Scheme 2, it can be seen, among the furans (they are the most used hole scavengers), that (A) 5-hydroxymethyl-2-furfural (HMF) gives rise to 2,5-furandicarboxaldehyde, also called 2,5-diformylfuran (FDC), and 2,5-furandicarboxylic acid (FDCA), while (B) furfuryl alcohol is partially oxidized to furfural and furoic acid.



Scheme 2. Oxidation pathways of 5-hydroxymethyl-2-furfural (HMF) (A) and furfuryl alcohol (B) to their corresponding aldehydes and acids.

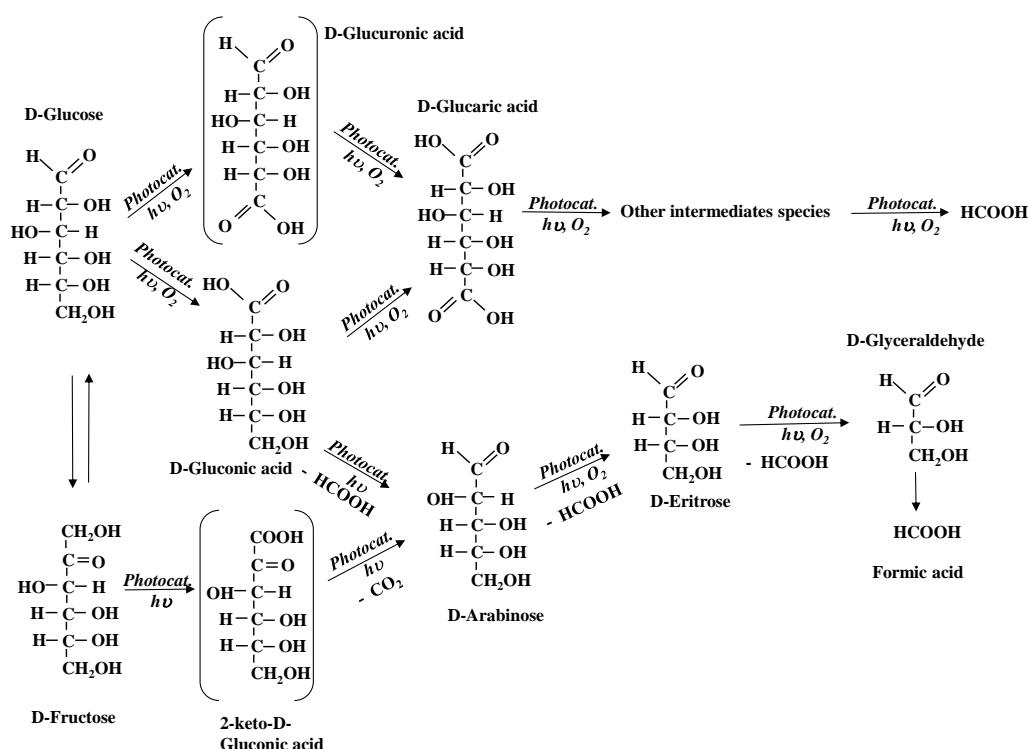
Furfural and 5-hydroxymethyl-2-furfural (HMF) are extensively accessible biomass-derived renewable chemical feedstocks, and their oxidation to 2,5 furandicarboxylic acid (FDCA) and furoic acid, respectively, is a research area with great possibilities for application in cosmetics, food, optics, and polymer industries. Water-based oxidation of furfural/HMF is a cost-effective approach to generating, at the same time, H_2 and furoic acid/FDCA. Nevertheless, this process is today limited to (photo)electrochemical methods that can be difficult to improve and scale up.

A wide range of biomass-derived compounds bearing a large variety of oxygen-containing functionalities can be used as a hole scavenger in the PR reaction, the most widely used being methanol, ethanol, and glycerol, but also aldehydes and alcohols of various kinds [13,14], saccharides [15] and others, such as amines [15] as triethanolamine (TEOA), or polysaccharides, including cellulose [16]. Monosaccharides, such as pentoses (ribose, arabinose) and hexoses (glucose, galactose, fructose, mannose), and organic acids (acetic acid, formic acid) have also been extensively used as hole scavengers [17].

Based on the species analyzed in an aqueous solution during the glucose PR, we hypothesized the reaction sequence reported in Scheme 3. Glucose was transformed into arabinose by α -cleavage in the presence of H_2O producing equimolar amounts of formic acid and H_2 , and subsequently, arabinose into erythrose by the same mechanism. The greater quantity of H_2 compared to formic acid can be explained by taking into account that its formation comes not only from glucose degradation but also from the splitting of water [18].

Di- or polysaccharides show that the hydrogen production rate is one or two orders of magnitude higher with respect to those reached in the presence of pure water [19].

The oxidation of the organic species has been considered unselective; however, some reports conclude that the organic molecules can be partially oxidized instead of mineralized, so PR for H_2 production can be more widely considered as a synthesis process where, for instance, alcohol is selectively oxidized to an aldehyde [9,20,21].



Scheme 3. Reaction pathway by using glucose as a hole scavenger in H₂ generation in the presence of Pt-TiO₂ photocatalysts in the anaerobic system [18].

Di- or polysaccharides show that the hydrogen production rate is one or two orders of magnitude higher with respect to those reached in the presence of pure water [19].

The oxidation of the organic species has been considered unselective; however, some reports conclude that the organic molecules can be partially oxidized instead of mineralized, so PR for H₂ production can be more widely considered as a synthesis process where, for instance, alcohol is selectively oxidized to an aldehyde [9,20,21].

Importantly, not all organic species are equally valid for this role, as Mills et al. pointed out. Organic species need to possess a suitable functional group (e.g., alcohol, carbonyl) and a hydrogen atom in the “ α ” position with respect to them [22]; organics without the alpha hydrogen, such as ketones and carboxylic acids, may result ineffective in PR.

Catalysis is among the principles of green chemistry [23], and together with the paradigm of obtaining a high reaction efficiency, assessed by the chemical yield, waste minimization is also one of the principles considered to support environmental sustainability [24], along with the energy expended in a process and the type of the catalysts that must be non-polluting. In this context, not only materials derived from waste are gaining more attention in recent years, but also the use of waste itself with a view to promoting a circular economy.

In a remarkable process, real biomass feedstocks can be used as hole scavengers in the PR reaction; raw feedstocks, such as wood, rice husks, sawdust, and algae, have been used in PR [25]. Lignocellulosic and agro-industrial waste and residues represent important feedstock for modern biorefineries aimed at the sustainable production of renewable energy and chemicals [26]. The most important biomass feedstocks are of three types: (i) lignocelluloses, (ii) starch-and sugar-based crops, (iii) vegetable oil crops [27], being the lignocellulosic substrates those present in greater quantities in the biosphere.

Lignocellulose is the biomass most abundant, and as illustrated in Figure 2, it is a combination of carbohydrate polymers (cellulose and hemicellulose) and aromatic polymers (lignin), including all dry waste derived from plants (biomass); moreover, it has an evolved structure to provide mechanical and chemical stability [28].

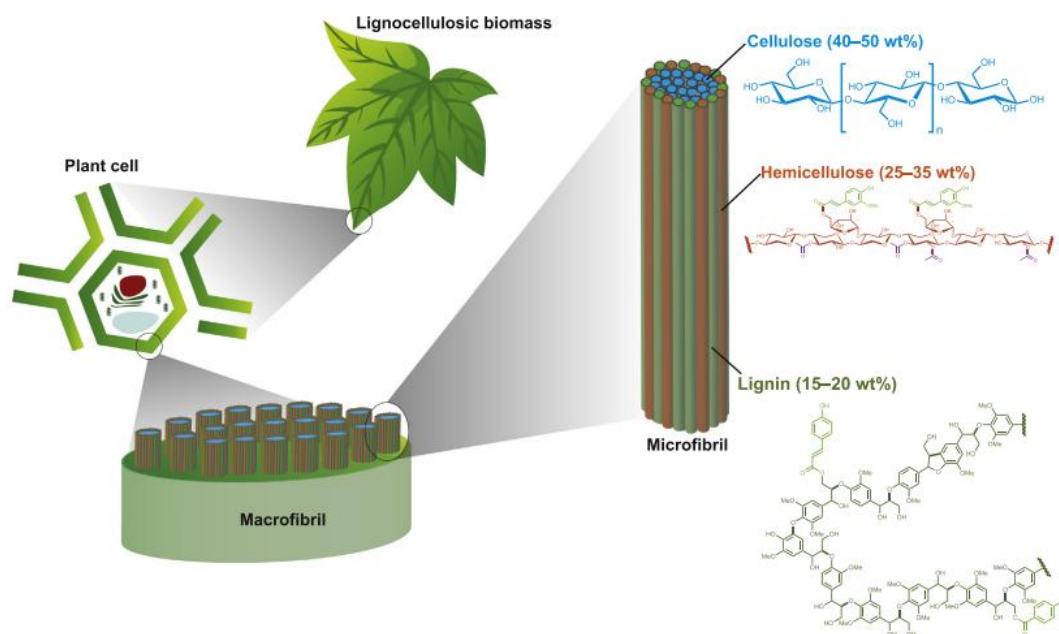


Figure 2. Schematic illustration of the chemical and spatial structure of lignocellulose. Reprinted with permission from Ref. [28]; © 2020 reprinted with permission from Elsevier.

Cellulose and hemicellulose are formed by long chains of hexose and pentose sugars such as $C_6H_{12}O_6$ or $C_5H_{10}O_5$, which can be easily photo-reformed by virtue of their polarity and the high content of hydroxyl groups ($-OH$), as shown in Figure 2. Lignin (also called lignocellulose) is a heavy and complex organic polymer consisting mostly of phenolic compounds, mainly found in the cell wall of plants. It is a polymer chain composed of phenylpropane molecules. Cellulose and lignin represent about 70% of the total biomass.

The content of chemical species varies significantly depending on the type of biomass selected. For example, considering biomass from food waste, cereals contain 70–80% carbohydrates (they represent very suitable biomass for photoreforming), while meat consists mainly of proteins and fats, both of which are unsuitable to be used in H_2O -based PR because of their structural complexity and hydrophobicity. Sugars were extensively studied as probe substrates for biomass PR since, as mentioned above, most of the biomass is based on saccharide chains (cellulose and hemicellulose). The most consolidated PR of glucose is carried out in the presence of TiO_2 [18]. An increase in temperature from 30 to 60 °C improved the H_2 production.

Chemisorbed biomass consumes all of the reactive oxygen species (ROS) produced in the photocatalytic process (h^+ , $\cdot OH$, O_2^- and 1O_2), generating the corresponding oxidized species in the PR reaction. In general, as an example, a monosaccharide as glucose generates small acidic species as lactic acid by isomerization, retro-aldol reaction, and dehydration [29]. Moreover, the cleavage of one C-C bond could give rise to a succession of arabinose, erythrose, and formic acid products in photocatalytic glucose partial oxidation and hence in reforming [30].

Disaccharides (maltose, sucrose, lactose) generally provided worse results than monosaccharides. The PR of soluble polysaccharides occurred at smaller H_2 yields, probably because of their high molecular weights and the presence of hydrogen bonds in the structures. The use of lignocellulose in PR is energy-demanding, because it requires the breaking of its structure. Depending on the kind of biomass chosen, the accessible chemical content for the PR is 55–95% by weight [31]. This percentage could increase with the incessant progress in photocatalytic materials able to photoreforming lignin, which, however, being a complex polymer, remains difficult to photo-reformate. Lignocellulose PR technology is still not suitable for the industrial expectations of the difficulty in the deconstruction of lignocellulosic feedstocks. In fact, the complex structure is difficult to be degraded and protect

against microbial attack. Moreover, the strong hydrogen bonds between the chains within the cellulose microfibrils make lignocellulose recalcitrant to chemical transformation.

As pointed out by Uekert, before using it for PR, the biomass feedstocks in general must suffer a pre-treatment. In the first stage, a mechanical treatment would produce small pieces; hence, a chemical pre-treatment would solubilize the organics to facilitate the contact between the hole scavenger and the photocatalyst during the PR, increasing the H_2 evolution rate. Some reports are devoted to the hydrolysis and solubilization at acidic or alkaline pHs, exposition of the feedstock to high-pressure saturated steam, enzymatic processes (mainly to hydrolyze cellulose) or others; however, no systematic study has been devoted to this important stage as far as the research has been focused on synthetic aqueous solutions of model molecules [32].

3. Some Considerations and Details on g-C₃N₄-Based Photocatalysts for H₂ Production

3.1. g-C₃N₄ as Photocatalyst

The ideal photocatalyst in a PR reaction should be selective versus the most value-added species deriving from organics oxidation, stable and cheap in order to be used on an industrial scale. Important parameters are band edges, optical absorbance, and carrier mobility. The biggest challenge for a photocatalyst is to possess suitable visible light absorption in order to harvest solar light and high carrier mobility, i.e., reduced recombination. Many semiconductors have been studied as photocatalysts, but certainly, TiO₂ has been the most studied due to its activity along with cost-effectiveness, safety, and (photo)chemical stability.

In the last decades, polymeric carbon nitride, known as melon, C₃N₄ polymer, or g-C₃N₄, has successfully been employed in photocatalysis due to its low cost, non-toxicity, thermal stability, appropriate band gap, and suitable photocatalytic performance. g-C₃N₄ consists of a conjugated polymeric system. Indeed, it is constituted by s-triazine or tri-s-triazine units interconnected via tertiary amines. The atoms in the layers are arranged in honeycomb configurations with strong covalent bonds. Interactions between the two-dimensional sheets (2D) are weak van der Waals forces. This material is highly stable in various solvents, including H₂O, diethylether, acetic acid, alcohols, N,N-dimethylformamide (DMF), toluene, tetrahydrofuran (THF), and NaOH aqueous solution. The g-C₃N₄ can be prepared by thermal condensation of nitrogenous precursors such as melamine, urea, thiourea, cyanamide, dicyandiamide, and ammonium thiocyanate. From these precursors, the organic moiety is transformed stepwise by slow calcination into the yellow-brown melon structure based on tri-s-triazine (heptazine) rings. Poly-addition and poly-condensation reactions occur together in a continuous manner to build the melon sheets that constitute the g-C₃N₄ structure [33]. As shown in Figure 3A, melon is structurally related to the more condensed (fully dehydrogenated) graphitic carbon nitride, g-C₃N₄, a visible-absorbing semiconductor. Melon, a highly ordered polymer, is the first formed polymeric g-C₃N₄ structure. Further reaction leads to more condensed and less defective g-C₃N₄ species, based on tri-s-triazine (C₆N₇) units as elementary building blocks. Melamine, melem, and melon are triazine- and heptazine (tri-s-triazine unit)-based molecular compounds to prepare g-C₃N₄. As illustrated in Figure 3B, triazine (C₃N₃) and heptazine (C₆N₇) rings are the basic tectonic units of g-C₃N₄.

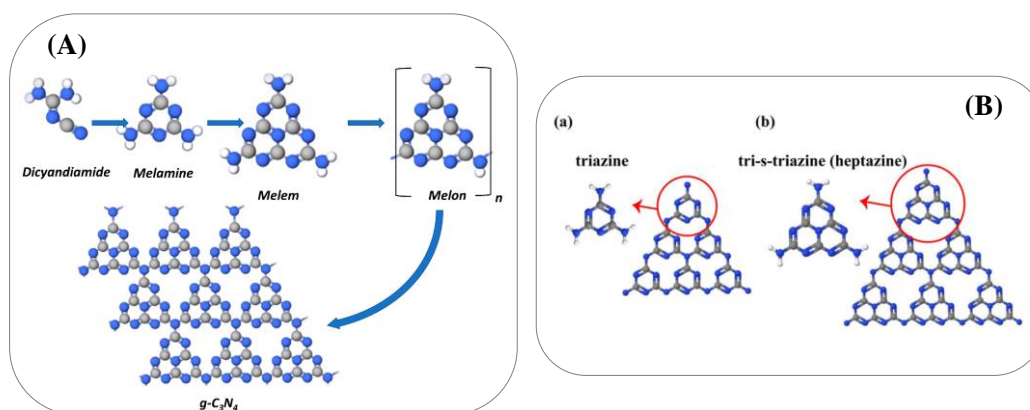


Figure 3. (A) Structures of melem, melon, and g-C₃N₄ obtained from the thermal condensation of dicyandiamide to form g-C₃N₄. Reprinted with permission from Ref. [34]; © 2023 MDPI. (B) (a) Triazine and (b) tri-s-triazine (heptazine) structures of g-C₃N₄ (gray, blue, and white balls are carbon, nitrogen, and hydrogen, respectively). Reprinted with permission from Ref. [35]; © 2022 MDPI.

Antonietti's group introduced this metal-free semiconductor in 2006 as a catalyst [36] and then, in 2009, as a heterogeneous photocatalyst for H₂ evolution [37]. It has been used as a photocatalyst for selective redox transformations [9,38]; indeed, the potential of the valence band (VB) and the absence of hydroxyl groups on the surface hinders the direct formation of ·OH radicals, species responsible for unselective oxidation of substrates. The HOMO-LUMO gaps of melem, polymeric melon (the building unit of g-C₃N₄), and an infinite sheet of a hypothetically fully condensed g-C₃N₄ were 3.5, 2.6, and 2.1 eV, respectively [37]. The calculated band gap of polymeric melon is very close to the experimentally measured medium-band gap of 2.7 eV, as reported by Antonietti et al., with the edges of the conduction band and valence band lying at −1.13 V and +1.57 V (vs. NHE at pH = 7) [39].

The photocatalytic activity of C₃N₄ has been hampered by several important drawbacks that are challenging to overcome, as evidenced in Figure 4; in particular, low charge carrier mobility and the fast recombination of the charge carriers restrict its practical use very significantly.

Several methods have been explored to modify/improve/optimize the structure of C₃N₄ by top-down strategies such as acid treatment, exfoliation, or etching, as well as bottom-up approaches [40]. Some synthetic strategies, such as nanostructure design, for instance, by using soft or rigid templates, electronic structure alteration via incorporation of dopant atoms, generation of point defects via vacancies, or the supramolecular pre-organization, allow to increase their specific surface area and to modify the value of the band gap. Furthermore, the deposition of noble metals and the construction of composites can improve the electron-hole separation, as will be better described below [41].

3.2. g-C₃N₄ in Anaerobic Conditions: Strategies to Improve Its Photocatalytic Activity

g-C₃N₄ has been used as a photocatalyst for water photo-splitting for the first time to obtain H₂ and O₂ under visible light irradiation by Antonietti's group [37]. The production of H₂ from an aqueous solution of triethanolamine (10 vol%) after 72 h of reaction passed from 7 to 770 µmol when 3 wt% of Pt nanoparticles were added to the bare semiconductor under irradiation with a wavelength longer than 420 nm. On the other hand, under UV irradiation at λ > 300 nm, the total H₂ production in 19 h was ca. 4.5 mmol in the presence of Pt/g-C₃N₄ photocatalyst.

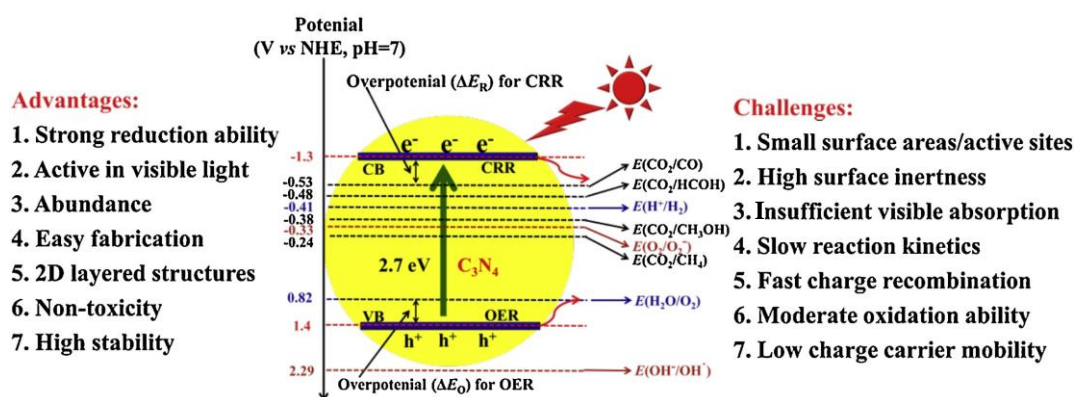


Figure 4. Advantages and disadvantages of g-C₃N₄ in photocatalysis along with the estimated position of the g-C₃N₄ band edges at pH 7 and reduction potentials of the relevant reactions related to water splitting and CO₂ reduction. Reprinted with permission from Ref. [41]; © 2017 Elsevier.

Very few papers report the evolution of H₂ from H₂O without the use of a hole scavenger. Ong et al. report only one example in the presence of a composite of g-C₃N₄/polypyrrole [42]. Polypyrrole injects electrons into the g-C₃N₄ conduction band, and the holes in the valence band of g-C₃N₄ react with water giving rise to H₂O₂. The authors do not propose a trap for polypyrrole valence band holes, which could hardly be transferred to solution species; hence, a self-oxidation of the polymer (sacrificial agent) would likely occur [43]. Alternatively, Liu et al. report O₂ and H₂ evolution in the absence of scavengers using as photocatalyst metal-free carbon nanodot/g-C₃N₄ nanocomposite. They calculated quantum efficiencies of 16% (at $\lambda = 420$ nm), 6.3% ($\lambda = 580$ nm), and 4.4% ($\lambda = 600$ nm) and obtained an overall efficiency in the solar energy conversion equal to ca. 2.0%. The mechanism of water oxidation is a process with two 2-electron steps yielding firstly H₂O₂ that subsequently decomposes to provide O₂ and H₂O. The rate increases with carbon nanodot loading because they catalyze the rate-limiting step, i.e., the H₂O₂ decomposition [44]. The results reported by Liu et al. are surprisingly high.

Generally, a hole scavenger is employed to minimize electron-hole recombination, often with suitable quantum yields, as reviewed by Naseri et al. [45], but as claimed before, the reaction cannot be considered water photo-splitting, but it regards the PR of the scavenger employed. The oxidation reaction is the rate-determining step of the overall reaction, so the use of electron donors (hole scavengers) clearly improves the activity [46].

In order to increase the catalytic activity of the pristine material, other additional strategies aimed at improving the absorption of visible light, reducing the electron-hole recombination rate, and improving the reaction kinetics have been extensively investigated. Such approaches include nanostructure architecture, doping, heterojunction, and the use of plasmonic metals and co-catalysts.

Noble metals such as Rh, Au, Ag, and particularly Pt are often used as co-catalysts because the metals trap photogenerated electrons as well as decrease the overpotential facilitating multielectron transfer reactions. Often, RuO₂ is also present to sink the holes, avoiding the photoproduct couples (h⁺/e⁻) recombination [47]. The large work function and low activation energy of Pt allow this metal to be the most effective cocatalyst for H₂ evolution [48]. The optimal amount of Pt follows a bell shape because the photocatalytic activity increases with increasing the amounts of metal. However, further increasing could lead to a decrease in the number of surface active sites on the semiconductor photocatalyst and even to a shielding effect on the incident light, as well as can favor electron/hole recombination, acting the metal as a recombination center. Furthermore, the presence of noble metal nanoparticles on the semiconductor surface can generate visible activated surface plasmon resonance (SPR) to activate the photocatalytic process to visible light irradiation.

Battula et al. report that Pt-C₃N₄ exhibited high selectivity to 2,5-diformylfuran (DFF) during the partial oxidation of 10 mL of an aqueous solution of 5-hydroxymethyl furfural

(10 mM) [49]. The obtained results are modest in terms of photoreforming, and a H_2 production rate of $12 \mu\text{mol h}^{-1} \text{m}^{-2}$ (corresponding to $2040 \mu\text{mol h}^{-1} \text{g}_{\text{cat}}^{-1}$) was obtained with a DFF yield of 13.8% with >99% selectivity after 6 h under simulated solar light (light intensity of 100 mW cm^{-2}) light. The selectivity was maintained even after 48 h of experiment, with an improved DFF yield of 38.4% and H_2 production rate of $36 \mu\text{mol h}^{-1} \text{m}^{-2}$ (corresponding to $6120 \mu\text{mol h}^{-1} \text{g}_{\text{cat}}^{-1}$).

Transition metals such as Fe, Co, and Ni or inorganic compounds such as $(\text{OH})_2$, MoS_2 , WS_2 , NiS, NiO, $\text{Ni}(\text{OH})_2$, or CoP have also been used as co-catalysts for the PR. The analogous layered structures of inorganic semiconductors, such as MoS_2 and g- C_3N_4 , gave rise to a composite that remarkably increased the photocatalytic H_2 evolution. This performance has been attributed to the similar layered geometries of the solid photocatalysts, which allow the composite to improve the mobility of charge carriers at the interfaces and hence their lifetime [50]. Interestingly, it was observed that by increasing from 0D to 1D, to 2D, and to 3D, the dimensions of conjugated polymers, the mobility of electrons rises, and, at the same time, the binding energies of the bound electron/hole pairs are reduced. For instance, it has been observed a decrease in the electron/hole recombination rate in the presence of graphene nanosheets/g- C_3N_4 composite for the photocatalytic H_2 evolution. Xiang et al. observed that an amount of 1 wt% of graphene on g- C_3N_4 was an optimum during the photoreforming of an aqueous solution of methanol carried out under visible light irradiation ($\lambda > 400 \text{ nm}$). In fact, the quantity of H_2 resulted ca. three-fold that found by using the pristine g- C_3N_4 . The heterojunction between g- C_3N_4 and graphene increases the electrical conductivity and improves the carrier separation. It is also capable of storing and transporting electrons to the reaction sites [51].

Improved performance for photocatalytic H_2 production has been reported by Sun et al., who highlighted the synergistic effect of rGO nanosheets and Pt nanoparticles. In fact, the rGO nanosheets, which act as electron transfer mediators, capture the electrons photo-generated by g- C_3N_4 and then transfer them to the Pt cocatalyst, while the nanoparticles of Pt act as reduction active sites to promote the H_2 evolution reaction [52].

In addition, Yan et al. report that in the composites g- C_3N_4 /rGO, the carbon nitride plays the role of the photocatalyst, whereas reduced graphene oxide can collect and transport electrons to reaction sites improving in this way the activity [53]. Organic polymers as poly(3-hexylthiophene) can exhibit semiconducting properties (band gap ca. 2 eV), and its composite with g- C_3N_4 , using Pt as cocatalyst, has been used for H_2 production from aqueous ascorbic acid under visible light irradiation [54]. The poly(3-hexylthiophene)/g- C_3N_4 composite enabled outstanding activities ($>300 \text{ mmol h}^{-1} \text{g}_{\text{cat}}^{-1}$) for irradiation with $\lambda > 500 \text{ nm}$. Although deactivation leading to 30% lower H_2 production rates after several days of operation has been observed, these results encourage further investigation of this inexpensive carbon-based material.

Interestingly, sunlight can also be used as an irradiation source to obtain H_2 from water by triethanolamine PR using rGO nanosheets/ C_3N_4 composites. The highest H_2 production observed on Ag-loaded samples (the wt% of Ag in the catalyst was in the range of 1–5%) was $525 \mu\text{mol h}^{-1} \text{g}_{\text{cat}}^{-1}$, which increased to ca. $88 \text{ mmol h}^{-1} \text{g}_{\text{cat}}^{-1}$ when 1 wt% of Pt was also present. The apparent quantum efficiency (AQE) reported for the best material was ca. 9% using, as an irradiation source, indifferently visible LED or natural sunlight [55].

Spinel ferrite-g- C_3N_4 systems also take advantage of sunlight for H_2 generation through PR [56]. For instance, the evolved H_2 rate by a ferrite-g- C_3N_4 composite gave rise to 10 times more H_2 than with the bare g- C_3N_4 . The efficiency of the composite was justified by claiming its optimized light absorption ability [57].

As far as composite semiconductor materials are concerned, an interesting idea is the Z-scheme. Bard suggested the first mechanism proposal of this system in 1979 [58]. It involves the transfer of electrons from the LUMO of the CB of WO_3 to the HOMO of the VB of C_3N_4 , thus gaining the capability to react for both electrons and holes compared to heterojunctions [59]. Few Z-scheme has been published in PR [60–62]. In the Z-scheme

g-C₃N₄/WO₃ published by Yu et al., a host-guest concept is conceived. Authors introduce WO₃ nanocuboids in the host g-C₃N₄ achieving an intimate interfacial contact with an injection of electrons from the WO₃ conduction band (CB) to the valence band (VB) of g-C₃N₄, as reported in Figure 5 [62]. The photocatalytic H₂ production was evaluated by using an aqueous solution of triethanolamine, which acted as a hole scavenger under simulated solar irradiation. The presence of 1 wt% Pt on g-C₃N₄ gave rise to an H₂ amount of 0.44 mmol h⁻¹ g_{cat}⁻¹. Indeed, the electrons from the CB of g-C₃N₄ (ca. -1.1 V vs. NHE) possess enough reducing power for the H₂ production, whereas pristine WO₃ resulted in virtual inactivity. The use of g-C₃N₄/WO₃ as a photocatalyst significantly enhanced the H₂ production to 3.12 mmol h⁻¹ g_{cat}⁻¹, i.e., it increased seven times [62].

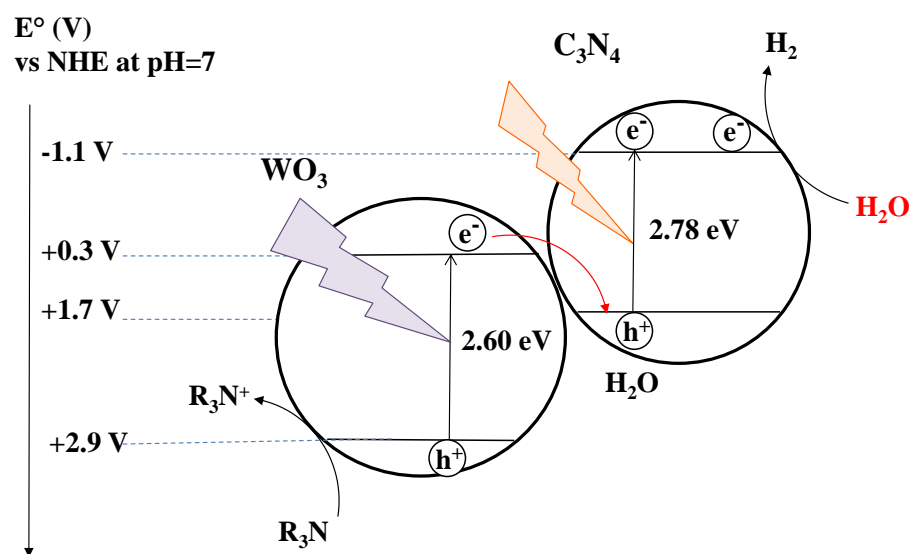


Figure 5. Z-scheme of visible light harvesting g-C₃N₄/WO₃ nanocomposite. CB and VB energy levels have been taken from [62].

Composites of Nb₂O₅/g-C₃N₄ exhibited high visible light absorption resulting in a notable photocatalytic activity under simulated sunlight irradiation using triethanolamine or methanol as hole scavengers. An amount of 110 mmol h⁻¹ g_{cat}⁻¹ of H₂ has been produced using a sample containing 10 wt% of g-C₃N₄ over niobium oxide, more than double that obtained with the pristine semiconductor [63]. The enhanced photocatalytic activity has been attributed to the energy and the fast separation of photogenerated electron-hole pairs at the Nb₂O₅/g-C₃N₄ interface through a direct Z-scheme, as suggested in Figure 6.

3.3. Real Wastes as Hole Scavengers in the Photoreforming Process in the Presence of g-C₃N₄-Based Semiconductors

The use of real biomass has been very rarely reported in the context of photoreforming technology, particularly in the presence of g-C₃N₄-based materials as photocatalysts. Uekert et al. have been the most active group, and pioneer, as far as we know, in using real waste in this process. It is interesting to mention that they have used not only biomass but real food wastes and synthetic polymers as hole scavengers. As well known, polymers are of particular concern due to their non-biodegradability and accumulation in the environment. In addition, plastics can be used in PR even if its oxidation is not a simple task because non-biodegradable polymers are composed of long hydrocarbon chains such as polyethylene or polystyrene, which are difficult to reform due to the stability of their C-C bonds [9,64]. Uekert et al. have studied this problem and proposed the use of carbon nitride/nickel phosphide composite as a photocatalyst to obtain H₂ by the PR of poly(ethylene-terephthalate) (PET) and poly(lactic acid) (PLA) under alkaline aqueous conditions [65]. They used as photocatalysts a cyanamide-functionalized carbon nitride

(CN_x) coupled with a nickel phosphide (Ni₂P). The same group has previously used bare C₃N₄ for lignocellulose PR [66]. They compared the activity of this material with that of CdS/CdO_x quantum dots in an alkaline aqueous solution via solar illumination at room temperature producing H₂ [67]. These authors have proven that glucose, fructose, galactose, sucrose, but also raw biomass such as starch, casein, bovine serum albumin (BSA), glycerol, castor oil, and soybean oil are suitable hole scavengers in PR by using photocatalysts both CdS/CdO_x in alkaline medium (KOH 10M) and the composite containing C₃N₄ in aqueous suspension, i.e., H₂NCN_x/Ni₂P. They observed that simple soluble molecules such as sugars, glutamic acid, and glycerol gave rise to the highest yields of H₂, though the activity decreased when the molecule to be oxidized became more complex. The same research group has also focused on the interesting aim of developing the use of food waste in PR. They argue that food waste PR can be applied to small off-grid systems to simultaneously handle food waste and generate H₂. Both CdS/CdO_x in an alkaline solution and the C₃N₄-based composite H₂NCN_x/Ni₂P at neutral pH have been active in this task [32]. Uekert et al. have selected casein, fructose, and starch as case studies because they are present in commonly discarded foods (bread, cheese, and apples). After 5 days of irradiation, conversions in H₂ with CdS/CdO_x in KOH were ca. 16–27% measured with respect to the theoretical yield of hydrogen, whereas they were 3–7% in the presence of the C₃N₄-based photocatalyst in KOH and 1–4% in water [32].

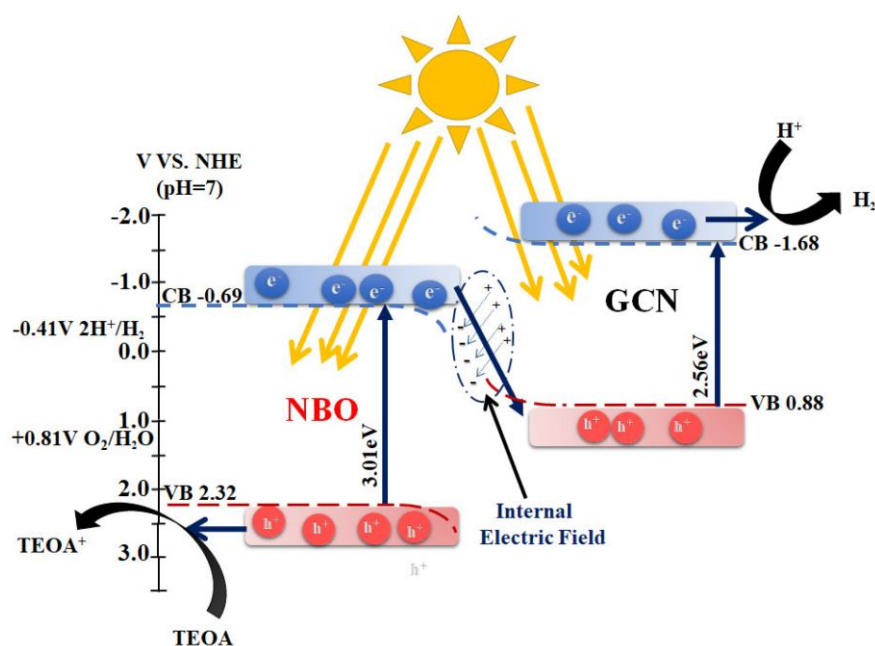


Figure 6. Scheme of the possible photocatalytic mechanism in the presence of Nb₂O₅/g-C₃N₄ photocatalysts. Reprinted with permission from Ref. [63]; © 2019 MDPI.

In any case, the most abundant renewable resource for the production of aromatic chemicals remains lignin, the natural amorphous polymer that acts as the essential glue that gives plants their structural integrity, which constitutes 15–30% by weight of the biomass [68]. Lignin mainly contains C–O bonds and C–C bonds, wherein the β -O-4 bond represents the main content [69,70]. The latter bond can be broken into more chemically useful fragments. Lignin can be converted into different aromatic compounds, which are in turn used to synthesize other value-added chemicals [21,31,70] and is able to produce H₂ in the order of mmol h^{−1} g_{cat}^{−1} [9,19,55].

4. Conclusions

Hydrogen production by photocatalysis in the presence of renewable solar energy is one of the most versatile and environmentally benign paths for research to pursue.

Photoreforming offers a simple, sunlight-driven method for transforming biomass waste into valuable chemicals and clean H₂ fuel. In this manner, H₂ can be produced at room temperature and atmospheric pressure by a simple, efficient, low-cost, and sustainable process, with the use of a heterogeneous photocatalyst using biomass, solar light, and water. Photoreforming involves the splitting of water to generate H₂ through a reduction reaction and the simultaneous oxidation of an organic species to obtain other molecules with higher added value or, simply, to completely oxidize (mineralize) organics to CO₂ and H₂O. The current manuscript overviews some of the most relevant studies focused on photoreforming using g-C₃N₄-based materials. Almost all of them report the use of model organic molecules as hole scavengers, considering them as biomass prototype species to investigate the photoreforming process at bench scale in order to understand the physical-chemical features of the process. The published studies have demonstrated that the PR of biomass is a promising approach to the sustainable generation of H₂ and feedstock chemicals. The simplicity of this process, which is capable of producing clean H₂ also at room temperature, is of considerable advantage if compared to thermochemical methods, but efficiencies are still lower than those of conventional processes. The use of g-C₃N₄ has been explored due to the several advantages in terms of cost, atoxicity, and thermodynamic constraints. Indeed, it has been demonstrated that g-C₃N₄ is able to work as a photocatalyst also under visible light irradiation. However, numerous disadvantages have also emerged, as concerns about its use as a pristine solid due to the high recombination rate of e⁻/h⁺ couples and the low oxidant capability of its valence band. The use of heterojunctions has been proposed as the best strategy to take advantage of the g-C₃N₄ potentialities, particularly in the presence of semiconductor oxides. The latter types of materials are particularly promising for PR reactions. In the future, a more transversal and interdisciplinary approach will be necessary in order to jump into the view of the use of real waste, currently pioneered faced by very few groups, as Uekert et al. In perspective, future studies should focus on the development of narrow band-gap materials to enhance solar energy conversion efficiency and to lower the required driving force, improving the selectivity toward high-value products. Furthermore, the use of real waste as hole scavengers would be approached. Photoreforming offers a unique sunlight-driven platform for transforming biomass waste resources, even when combined with other types of waste, into both valuable H₂ and organic chemicals. To this aim, an intense dialogue among chemists, materials science scientists, engineers, and technologists is mandatory.

Author Contributions: Conceptualization, E.I.G.-L., L.P. and G.M.; methodology, E.I.G.-L. and G.M.; software, E.I.G.-L. and G.M.; investigation, E.I.G.-L. and G.M.; resources, E.I.G.-L., L.P. and G.M.; data curation, E.I.G.-L., L.P. and G.M.; writing—original draft preparation, E.I.G.-L.; writing—review and editing, E.I.G.-L., L.P. and G.M.; visualization, E.I.G.-L., L.P. and G.M.; supervision, L.P. and G.M.; project administration, G.M.; funding acquisition, L.P. All authors have read and agreed to the published version of the manuscript.

Funding: This research received no external funding.

Data Availability Statement: No further data available.

Conflicts of Interest: The authors declare no conflict of interest.

References

1. Ng, C.H.; Teo, S.H.; Mansir, N.; Islam, A.; Joseph, C.G.; Hayase, S.; Taufiq-Yap, Y.H.; Yap, T. Recent advancements and opportunities of decorated graphitic carbon nitride toward solar fuel production and beyond. *Sustain. Energy Fuels* **2021**, *5*, 4457–4511. [[CrossRef](#)]
2. DOE Hydrogen and Fuel Cells Program: 2014 Annual Progress Report; US Department of Energy: Washington, DC, USA, 2014.
3. Turner, J.A. Sustainable hydrogen production. *Science* **2004**, *305*, 972–974. [[CrossRef](#)] [[PubMed](#)]
4. García-López, E.I.; Palmisano, L. Chapter 1: Fundamentals of photocatalysis: The role of the photocatalysts in heterogeneous photo-assisted reactions. In *Materials Science in Photocatalysis*, 1st ed.; García-López, E.I., Palmisano, L., Eds.; Elsevier: Amsterdam, The Netherlands, 2021; pp. 3–9.

5. Fujishima, A.; Honda, K. Electrochemical Photolysis of Water at a Semiconductor Electrode. *Nature* **1972**, *238*, 37–38. [[CrossRef](#)] [[PubMed](#)]
6. Samage, A.; Gupta, P.; Halakarni, M.A.; Nataraj, S.K.; Sinhamahapatra, A. Progress in the Photoreforming of Carboxylic Acids for Hydrogen Production. *Photochemistry* **2022**, *2*, 40. [[CrossRef](#)]
7. Jitputti, J.; Pavasupree, S.; Suzuki, Y.; Yoshikawa, S. Synthesis and photocatalytic activity for water-splitting reaction of nanocrystalline mesoporous titania prepared by hydrothermal method. *J. Solid State Chem.* **2007**, *180*, 1743–1749. [[CrossRef](#)]
8. Kawai, T.; Sakata, T. Conversion of carbohydrate into hydrogen fuel by a photocatalytic process. *Nature* **1980**, *286*, 474–476. [[CrossRef](#)]
9. Toe, C.Y.; Tsounis, C.; Zhang, J.; Masood, H.; Gunawan, D.; Scott, J.; Amal, R. Advancing photoreforming of organics: Highlights on photocatalyst and system designs for selective oxidation reactions. *Energy Environ. Sci.* **2021**, *14*, 1140–1175. [[CrossRef](#)]
10. Al-Mazroai, L.S.; Bowker, M.; Davies, P.; Dickinson, A.; Greaves, J.; James, D.; Millard, L. The photocatalytic reforming of methanol. *Catal. Today* **2007**, *122*, 46–50. [[CrossRef](#)]
11. Romero Ocana, I.; Beltram, A.; Delgado Jaen, J.J.; Adami, G.; Montini, T.; Fornasiero, P. Photocatalytic H₂ production by ethanol photodehydrogenation: Effect of anatase/brookite nanocomposites composition. *Inorg. Chim. Acta* **2015**, *431*, 197–205. [[CrossRef](#)]
12. Daskalaki, V.M.; Kondarides, D.I. Efficient production of hydrogen by photo-induced reforming of glycerol at ambient conditions. *Catal. Today* **2009**, *144*, 75–80. [[CrossRef](#)]
13. Bahruji, H.; Bowker, M.; Davies, P.R.; Pedrono, F. New insights into the mechanism of photocatalytic reforming on Pd/TiO₂. *Appl. Catal. B* **2011**, *107*, 205–209. [[CrossRef](#)]
14. Bowker, M.; Morton, C.; Kennedy, J.; Bahruji, H.; Greaves, J.; Jones, W.; Davies, P.R.; Brookes, C.; Wells, P.P.; Dimitratos, N. Hydrogen production by photoreforming of biofuels using Au, Pd and Au-Pd/TiO₂ photocatalysts. *J. Catal.* **2014**, *10*, 10–15. [[CrossRef](#)]
15. Bowker, M.; Bahruji, H.; Kennedy, J.; Jones, W.; Hartley, G.; Morton, C. Photocatalytic Window: Photo-reforming of organics and water splitting for sustainable hydrogen production. *Catal. Lett.* **2015**, *145*, 214–219. [[CrossRef](#)]
16. Caravaca, A.; Jones, W.; Hardacre, C.; Bowker, M. H₂ production by the photocatalytic reforming of cellulose and raw biomass using Ni, Pd, Pt and Au on titania. *Proc. R. Soc. A* **2016**, *472*, 20160054. [[CrossRef](#)] [[PubMed](#)]
17. Ma, J.; Liu, K.; Yang, X.; Jin, D.; Li, Y.; Jiao, G.; Zhou, J.; Sun, R. Recent Advances and Challenges in Photoreforming of Biomass-Derived Feedstocks into Hydrogen, Biofuels, or Chemicals by Using Functional Carbon Nitride Photocatalysts. *ChemSusChem* **2021**, *14*, 4903–4922. [[CrossRef](#)]
18. Bellardita, M.; García-López, E.I.; Marci, G.; Palmisano, L. Photocatalytic formation of H₂ and value-added chemicals in aqueous glucose (Pt)-TiO₂ suspension. *Int. J. Hydrogen Energy* **2016**, *41*, 5934–5947. [[CrossRef](#)]
19. Huang, C.W.; Nguyen, B.S.; Wu, J.C.S.; Nguyen, V.H. A current perspective for photocatalysis towards the hydrogen production from biomass-derived organic substances and water. *Int. J. Hydrogen Energy* **2020**, *45*, 18144–18159. [[CrossRef](#)]
20. Wang, J.; Zhao, H.; Lui, P.; Yasri, N.; Zhong, N.; Kibria, M.G.; Hu, J. Selective superoxide radical generation for glucose photoreforming into arabinose. *J. Energy Chem.* **2022**, *74*, 324–331. [[CrossRef](#)]
21. Marci, G.; García-López, E.I.; Palmisano, L. Polymeric carbon nitride (C₃N₄) as heterogeneous photocatalyst for selective oxidation of alcohols to aldehydes. *Catal. Today* **2018**, *315*, 126–137. [[CrossRef](#)]
22. Bowker, M.; O'Rourke, C.; Mills, A. The Role of Metal Nanoparticles in Promoting Photocatalysis by TiO₂. *Top. Curr. Chem.* **2022**, *380*, 17. [[CrossRef](#)]
23. Anastas, P.T.; Warner, J.C. *Green Chemistry: Theory and Practice*; Oxford University Press: Oxford, UK, 1998.
24. Sheldon, R.A. Fundamentals of green chemistry: Efficiency in reaction design. *Chem Soc. Rev.* **2012**, *41*, 1437–1451. [[CrossRef](#)] [[PubMed](#)]
25. Butburee, T.; Chakthranont, P.; Phawa, C.; Faungnawakij, K. Beyond Artificial Photosynthesis: Prospects on Photobiorefinery. *ChemCatChem* **2020**, *12*, 1873–1890. [[CrossRef](#)]
26. Rodríguez-Padrón, D.; Puente-Santiago, A.R.; Balu, A.M. Environmental catalysis: Present and future. *ChemCatChem* **2019**, *11*, 18–38. [[CrossRef](#)]
27. Huber, G.W.; Iborra, S.; Corma, A. Synthesis of transportation fuels from biomass: Chemistry, catalysts, and engineering. *Chem. Rev.* **2006**, *106*, 4044–4098. [[CrossRef](#)] [[PubMed](#)]
28. Bertella, S.; Luterbacher, J.S. Lignin Functionalization for the Production of Novel Materials. *Trends Chem.* **2020**, *2*, 440–453. [[CrossRef](#)]
29. Zhao, H.; Li, C.; Yong, X.; Kumar, P.; Palma, B.; Hu, Z.; Tendeloo, G.; Siahrostami, S.; Larter, S.; Zheng, D.; et al. Coproduction of hydrogen and lactic acid from glucose photocatalysis on band-engineered Zn_{1-x}Cd_xS homojunction. *iScience* **2021**, *24*, 102109. [[CrossRef](#)]
30. Bellardita, M.; García-López, E.I.; Marci, G.; Megna, B.; Pomilla, F.R.; Palmisano, L. Photocatalytic conversion of glucose in aqueous suspensions of heteropolyacid-TiO₂ composites. *RSC Adv.* **2015**, *5*, 59037. [[CrossRef](#)]
31. Kuehnel, M.F.; Reisner, E. Solar Hydrogen Generation from Lignocellulose. *Angew. Chem. Int. Ed.* **2018**, *57*, 3290–3296. [[CrossRef](#)]
32. Uekert, T.; Pichler, C.M.; Schubert, T.; Reisner, E. Solar-driven reforming of solid waste for a sustainable future. *Nat. Sustain.* **2021**, *4*, 383–391. [[CrossRef](#)]
33. Muhmood, T.; Xia, M.; Lei, W.; Wang, F. Erection of duct-like graphitic carbon nitride with enhanced photocatalytic activity for ACB photodegradation. *J. Phys. D Appl. Phys.* **2018**, *51*, 065501. [[CrossRef](#)]

34. Zhurenok, A.V.; Vasilchenko, D.B.; Kozlova, E.A. Comprehensive Review on g-C₃N₄-Based Photocatalysts for the Photocatalytic Hydrogen Production under Visible Light. *Int. J. Mol. Sci.* **2023**, *24*, 346. [\[CrossRef\]](#) [\[PubMed\]](#)
35. Alaghmandfard, A.; Ghandi, K. A Comprehensive Review of Graphitic Carbon Nitride (g-C₃N₄)-Metal Oxide-Based Nanocomposites: Potential for Photocatalysis and Sensing. *Nanomaterials* **2022**, *12*, 294. [\[CrossRef\]](#) [\[PubMed\]](#)
36. Goettmann, F.; Fischer, A.; Antonietti, M.; Thomas, A. Metal-free catalysis of sustainable Friedel-Crafts reactions: Direct activation of benzene by carbon nitrides to avoid the use of metal chlorides and halogenated compounds. *Chem. Commun.* **2006**, *5*, 4530–4532. [\[CrossRef\]](#)
37. Wang, X.C.; Maeda, K.; Thomas, A.; Takanabe, K.; Xin, G.; Domen, K.; Antonietti, M. A metal-free polymeric photocatalyst for hydrogen production from water under visible light. *Nat. Mater.* **2009**, *8*, 76–80. [\[CrossRef\]](#)
38. Hollmann, D.; Karnahl, M.; Tschierlei, S.; Kailasam, K.; Schneider, M.; Radnik, J.; Grabow, K.; Bentrup, U.; Junge, H.; Beller, M.; et al. Structure-Activity Relationships in Bulk Polymeric and Sol–Gel-Derived Carbon Nitrides during Photocatalytic Hydrogen Production. *Chem. Mater.* **2014**, *26*, 1727–1733. [\[CrossRef\]](#)
39. Cui, Y.J.; Ding, Z.X.; Liu, P.; Antonietti, M.; Fu, X.Z.; Wang, X.C. Metal-free activation of H₂O₂ by g-C₃N₄ under visible light irradiation for the degradation of organic pollutants. *Phys. Chem. Chem. Phys.* **2012**, *14*, 1455–1462. [\[CrossRef\]](#) [\[PubMed\]](#)
40. Niu, P.; Zhang, L.; Liu, G.; Cheng, H. Graphene-like carbon nitride nanosheets for improved photocatalytic activities. *Adv. Funct. Mater.* **2012**, *22*, 4763–4770. [\[CrossRef\]](#)
41. Wen, J.; Xie, J.; Chen, X.; Li, X. A review on g-C₃N₄-based photocatalysts. *Appl. Surf. Sci.* **2017**, *391*, 72–123. [\[CrossRef\]](#)
42. Ong, W.J.; Tan, L.L.; Ng, Y.H.; Yong, S.T.; Chai, S.P. Graphitic Carbon Nitride (g-C₃N₄)-Based Photocatalysts for Artificial Photosynthesis and Environmental Remediation: Are We a Step Closer To Achieving Sustainability? *Chem. Rev.* **2016**, *116*, 7159–7329. [\[CrossRef\]](#)
43. Sui, Y.; Liu, J.; Zhang, Y.; Tian, X.; Chen, W. Dispersed conductive polymer nanoparticles on graphitic carbon nitride for enhanced solar-driven hydrogen evolution from pure water. *Nanoscale* **2013**, *5*, 9150–9155. [\[CrossRef\]](#)
44. Liu, J.; Liu, Y.; Liu, N.; Han, Y.; Zhang, X.; Huang, H.; Lifshitz, Y.; Lee, S.; Zhong, J.; Kang, Z. Metal-free efficient photocatalyst for stable visible water splitting via a two-electron pathway. *Science* **2015**, *347*, 970–974. [\[CrossRef\]](#)
45. Naseri, A.; Samadi, M.; Pourjavadi, A.; Moshfegh, A.Z.; Ramakrishna, S. Graphitic carbon nitride (g-C₃N₄)-based photocatalysts for solar hydrogen generation: Recent advances and future development directions. *J. Mater. Chem. A* **2017**, *5*, 23406–23433. [\[CrossRef\]](#)
46. Cao, S.; Low, J.; Yu, J.; Jaroniec, M. Polymeric photocatalysts based on graphitic carbon nitride. *Adv. Mater.* **2015**, *27*, 2150–2176. [\[CrossRef\]](#) [\[PubMed\]](#)
47. Yang, J.; Wang, D.; Han, H.; Li, C. Roles of cocatalysts in photocatalysis and photoelectrocatalysis. *Acc. Chem. Res.* **2013**, *46*, 1900–1909. [\[CrossRef\]](#) [\[PubMed\]](#)
48. Maeda, K.; Wang, X.; Nishihara, Y.; Lu, D.; Antonietti, M.; Domen, K. Photocatalytic activities of graphitic carbon nitride powder for water reduction and oxidation under visible light. *J. Phys. Chem. C* **2009**, *113*, 4940–4947. [\[CrossRef\]](#)
49. Battula, V.R.; Jaryal, A.; Kailasam, K. Visible light-driven simultaneous H₂ production by water splitting coupled with selective oxidation of HMF to DFF catalyzed by porous carbon nitride. *J. Mater. Chem. A* **2019**, *7*, 5643–5649. [\[CrossRef\]](#)
50. Hou, Y.; Laursen, A.B.; Zhang, J.; Zhang, G.; Zhu, Y.; Wang, X.; Dahl, S.; Chorkendorff, I. Layered nanojunctions for hydrogen-evolution catalysis. *Angew. Chem. Int. Ed.* **2013**, *52*, 3621–3625. [\[CrossRef\]](#)
51. Xiang, Q.; Yu, J.; Jaroniec, M. Preparation and Enhanced Visible-Light Photocatalytic H₂-Production Activity of Graphene/C₃N₄ Composites. *J. Phys. Chem. C* **2011**, *115*, 7355–7363. [\[CrossRef\]](#)
52. Sun, Q.; Wang, P.; Yu, H.G.; Wang, X.F. In situ hydrothermal synthesis and enhanced photocatalytic H₂-evolution performance of suspended rGO/g-C₃N₄ photocatalysts. *J. Mol. Catal. A* **2016**, *424*, 369–376. [\[CrossRef\]](#)
53. Yan, J.Q.; Peng, W.; Zhang, S.S.; Lei, D.P.; Huang, J.H. Ternary Ni₂P/reduced graphene oxide/g-C₃N₄ nanotubes for visible light-driven photocatalytic H₂ production. *Int. J. Hydrogen Energy* **2020**, *45*, 16094–16104. [\[CrossRef\]](#)
54. Zhang, X.H.; Peng, B.S.; Zhang, S.; Peng, T.Y. Robust Wide Visible-Light-Responsive Photoactivity for H₂ Production over a Polymer/Polymer Heterojunction Photocatalyst: The Significance of Sacrificial Reagent. *ACS Sustain. Chem. Eng.* **2015**, *3*, 1501–1509. [\[CrossRef\]](#)
55. García-López, E.I.; Lo Meo, P.; Megna, B.; Palmisano, L.; Marci, G. C₃N₄/reduced graphene oxide based photocatalysts for H₂ evolution from aqueous solutions of oxygenated organic molecules. *Catal. Today* **2022**, in press. [\[CrossRef\]](#)
56. Acharya, R.; Pati, S.; Parida, K. A review on visible light driven spinel ferrite-g-C₃N₄ photocatalytic systems with enhanced solar light utilization. *J. Mol. Liq.* **2022**, *357*, 119105. [\[CrossRef\]](#)
57. Jo, W.K.; Moru, S.; Tonda, S. Magnetically responsive SnFe₂O₄/g-C₃N₄ hybrid photocatalysts with remarkable visible-light-induced performance for degradation of environmentally hazardous substances and sustainable hydrogen production. *Appl. Surf. Sci.* **2020**, *506*, 144939. [\[CrossRef\]](#)
58. Bard, A.J. Photoelectrochemistry and heterogeneous photocatalysis at semiconductors. *J. Photochem.* **1979**, *10*, 59–75. [\[CrossRef\]](#)
59. Zhou, P.; Yu, J.; Jaroniec, M. All-Solid-State Z-Scheme Photocatalytic Systems. *Adv. Mater.* **2014**, *26*, 4920–4935. [\[CrossRef\]](#)
60. Yu, Z.B.; Xie, Y.P.; Liu, G.; Lu, G.Q.; Ma, X.L.; Cheng, H.M. Self-assembled CdS/Au/ZnO heterostructure induced by surface polar charges for efficient photocatalytic hydrogen evolution. *J. Mater. Chem. A* **2013**, *1*, 2773–2776. [\[CrossRef\]](#)
61. Fu, N.; Jin, Z.; Wu, Y.; Lu, G.; Li, D. Z-Scheme Photocatalytic System Utilizing Separate Reaction Centers by Directional Movement of Electrons. *J. Phys. Chem. C* **2011**, *115*, 8586–8593. [\[CrossRef\]](#)

62. Yu, W.; Chen, J.; Shang, T.; Chen, L.; Gu, L.; Peng, T. Direct Z-scheme g-C₃N₄/WO₃ photocatalyst with atomically defined junction for H₂ production. *Appl. Catal. B* **2017**, *219*, 693–704. [[CrossRef](#)]
63. Idrees, F.; Dillert, R.; Bahnemann, D.; Butt, F.K.; Tahir, M. In-Situ Synthesis of Nb₂O₅/gC₃N₄ Heterostructures as Highly Efficient Photocatalysts for Molecular H₂ Evolution under Solar Illumination. *Catalysts* **2019**, *9*, 169. [[CrossRef](#)]
64. Han, M.; Zhu, S.; Xia, C.; Yang, B. Photocatalytic upcycling of poly(ethylene terephthalate) plastic to high-value chemicals. *Applied Catal. B* **2022**, *316*, 121662. [[CrossRef](#)]
65. Uekert, T.; Kasap, H.; Reisner, E. Photoreforming of nonrecyclable plastic waste over a carbon nitride/nickel phosphide catalyst. *J. Am. Chem. Soc.* **2019**, *141*, 15201–15210. [[CrossRef](#)]
66. Kasap, H.; Achilleos, D.S.; Huang, A.; Reisner, E. Photoreforming of Lignocellulose into H₂ Using Nanoengineered Carbon Nitride under Benign Conditions. *J. Am. Chem. Soc.* **2018**, *140*, 11604–11607. [[CrossRef](#)] [[PubMed](#)]
67. Uekert, T.; Kuehnel, M.F.; Wakerley, D.W.; Reisner, E. Plastic waste as a feedstock for solar-driven H₂ generation. *Energy Environ. Sci.* **2018**, *11*, 2853–2857. [[CrossRef](#)]
68. Zakzeski, J.; Bruijninx, P.C.A.; Jongerius, A.L.; Weckhuysen, B.M. The Catalytic Valorization of Lignin for the Production of Renewable Chemicals. *Chem. Rev.* **2010**, *110*, 3552–3599. [[CrossRef](#)] [[PubMed](#)]
69. Shi, C.; Kang, F.; Zhu, Y.; Teng, M.; Shi, J.; Qi, H.; Huang, Z.; Si, C.; Jiang, F.; Hu, J. Photoreforming lignocellulosic biomass for hydrogen production: Optimized design of photocatalyst and photocatalytic system. *Chem. Eng. J.* **2023**, *452*, 138980. [[CrossRef](#)]
70. Liu, X.; Duan, X.; Wei, W.; Wang, S.; Ni, B.J. Photocatalytic conversion of lignocellulosic biomass to valuable products. *Green Chem.* **2019**, *21*, 4266–4289. [[CrossRef](#)]

Disclaimer/Publisher's Note: The statements, opinions and data contained in all publications are solely those of the individual author(s) and contributor(s) and not of MDPI and/or the editor(s). MDPI and/or the editor(s) disclaim responsibility for any injury to people or property resulting from any ideas, methods, instructions or products referred to in the content.